

Characterizations of porous titania thin films produced by electrochemical etching

S.K. Hazra^a, S.R. Tripathy^b, I. Alessandri^c, L.E. Depero^c, S. Basu^{a,*}

^a Materials Science Centre, Indian Institute of Technology, Kharagpur 721302, West Bengal, India

^b Institute of Materials Research and Engineering (IMRE), 3 Research Link, Singapore 117602, Singapore

^c Chemistry for Technologies Laboratory, University of Brescia, 25123 Brescia, Italy

Received 1 March 2006; received in revised form 6 April 2006; accepted 7 April 2006

Abstract

Porous titania templates were prepared by thermal oxidation followed by electrochemical etching. A thin layer (10 nm) of Ti–2 wt%Al was deposited on 0.25 mm titanium substrates having a thick (100 nm) gold coating on the back surface. The substrates were then thermally oxidized at 800 °C in 1% O₂/Ar ambience. Aluminium was used to dope the titanium dioxide films in order to increase the non-stoichiometry in the oxide matrix and hence the conductivity. The as-grown oxide was then electrochemically etched in 0.1 M dilute sulphuric acid medium under 10 V potentiostatic bias for 30 min. For photo-electrochemical etching the oxide samples were exposed to 400-W UV radiations. The crystalline composition of the as-oxidized and electrochemically etched samples was analyzed by glancing angle X-ray diffraction studies (GAXRD) at different incident angles (0.2°, 0.5°, 1.0° and 10°). The surface morphology was studied by scanning electron microscopy (SEM) and the rms roughness of the porous surfaces was obtained from atomic force microscopy (AFM) studies. Resistivity and Hall Effect experiments at room temperature revealed n-type semiconducting nature of the grown oxide. The sensor study with palladium catalytic contact showed high sensitivity and fast response in 500 and 1000 ppm hydrogen. The calculated response time in 1000 ppm hydrogen was 5 s at 300 °C.

© 2006 Elsevier B.V. All rights reserved.

Keywords: Photo-electrochemical etching; Porous titania; Stoichiometry; Surface roughness; Hydrogen sensor

1. Introduction

Titanium dioxide is a versatile material for different applications. It is used as heterogeneous catalyst, photocatalyst in solar cells, gas sensors and white pigments (in paints, cosmetics, etc.). Also it has electronic and electrical applications in MOS-FET (as a gate insulator) and varistors. It exists in three different polymorphs—brookite (orthorhombic), anatase and rutile (both tetragonal) [1]. Only anatase and rutile play significant role in various applications of TiO₂. Amongst the three phases, rutile titanium dioxide is the stable high temperature phase while the low temperature phases (brookite and anatase) are metastable. It is reported that the crystallographic phase change from anatase to rutile occurs in the temperature range 400–1200 °C [2]. The onset temperature and the rate of this transformation depend on a number of parameters like grain size, impurities, processing,

etc. Rutile TiO₂ thin films can be used both for low temperature and high temperature applications because the crystallographic phase change to rutile titanium dioxide is irreversible.

Titanium dioxide is also a fascinating material from a surface science point of view. Tailor made titania surfaces are very useful for different electronic applications especially as gas sensors and solar cells. The prime requirement for these important applications is high active surface area. Development of surface porosity is a convenient technique to increase the active surface area. The simplest approach to generate porosity is electrochemical anodic oxidation. Gong et al. [3] developed uniformly oriented porous titania nanostructures by anodic oxidation of high purity titanium in hydrofluoric acid medium under potentiostatic bias. In continuation to this work Varghese et al. [4,5] established the hydrogen sensitivity of these titania nanostructures both at high temperature and at room temperature. Recently, Paulose et al. reported ultra-high hydrogen sensitivity at room temperature using a unique architecture comprising of highly ordered undoped titania nanotube array [6]. The variation in electrical resistance, as reported by Paulose et al. [6], was

* Corresponding author. Tel.: +91 3222 283972, fax: +91 3222 255303.
E-mail address: sukumar_basu@yahoo.co.uk (S. Basu).

about 8.7 orders of magnitude (50,000,000,000%) when exposed to alternating atmospheres of nitrogen containing 1000 ppm of hydrogen and air at room temperature. Shimizu et al. [7] used dilute sulphuric acid to deposit TiO_2 thin films with nanoholes (at 30 °C) and studied the hydrogen sensitivity with palladium catalytic contact. Iwanaga et al. [8] further studied the hydrogen sensitivity of palladium contacted porous titania structures deposited at different temperatures. Porosity can also be generated in a titania matrix by potentiostatic electrochemical etching as well as potentiostatic photo-electrochemical etching. Sugiura et al. [9,10] fabricated TiO_2 nano-honeycomb structure in 0.1 M H_2SO_4 aqueous solution under a potentiostatic condition by illuminating the electrodes with a high-pressure mercury arc lamp for possible applications as photocatalysts and dye-sensitized solar cells.

In this study we report on the growth and characterizations of porous titania thin films by a novel route for possible applications as fast responding chemical gas sensors. A simple method was adopted to grow titanium dioxide thin films by thermal oxidation technique and then electrochemically etched in absence and also in presence of 400-W UV radiations separately. The crystalline composition of the samples along the depth of the oxide layer was checked by glancing angle X-ray diffraction studies (GAXRD) at different incident angles. The difference in the porous morphology attributed to the etched samples due to UV radiations was analyzed by scanning electron microscopy (SEM) and atomic force microscopy (AFM) experiments. The semiconducting parameters of the grown oxide samples were obtained from resistivity and Hall Effect experiments at room temperature. Finally, the porous titanium dioxide was used as micro/nanostructured templates to fabricate devices with palladium catalytic contact for fast responding hydrogen sensors.

2. Experimental

High purity titanium (99.7%) foil (0.25 mm thick) from M/S Sigma–Aldrich, USA, was the starting material for the growth of porous titania. Pieces of 5 mm × 5 mm were cut from the foil and one side was coated with gold (100 nm). On the other side a thin layer (10 nm) of Ti–2 wt%Al solid solution was deposited by e-beam evaporation at a base pressure of 4×10^{-6} mbar. The solid solution was prepared by mixing titanium metal with 2 wt% aluminium (99.9%) in a “Tungsten Inert Gas” (TIG) electric arc furnace. The materials were kept in a water-cooled copper hearth inside the TIG furnace. Oxygen was eliminated from the TIG furnace with the help of high vacuum facility attached to the furnace. Initially the pressure inside the furnace was reduced to 2×10^{-2} mbar using the rotary pump and then high purity argon was introduced to bring back to the normal atmospheric pressure. The furnace was again evacuated to 2×10^{-2} mbar pressure and purged with high purity argon. This procedure was repeated four times and then the pressure of the furnace was reduced to 8×10^{-6} mbar with the help of rotary and oil diffusion pump. Finally, the furnace chamber was filled with high purity argon to normal atmospheric pressure and the pumps were switched off. The electric arc was then generated from the tungsten tip to start mixing for solid solution. During mixing, a rotational motion

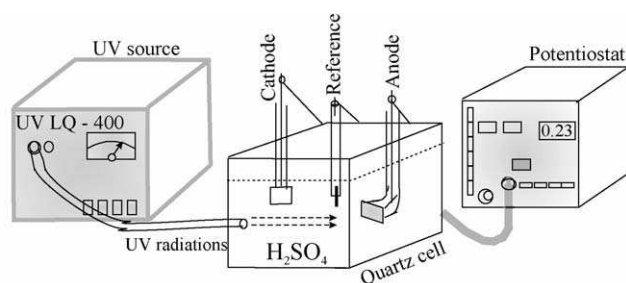


Fig. 1. Schematic drawing of the electrochemical etching setup.

was given to the molten mass by skillfully handling the electric arc to have a homogeneous solid solution. The mixing procedure was repeated five times after regular intervals to achieve uniformity in the solid solution.

The thin films on gold-coated titanium substrates were oxidized at 800 °C in 1% O_2/Ar ambient for 1 h to produce rutile titanium dioxide on the surface. Initially an inert atmosphere was maintained by flowing high purity argon until the temperature reached 800 °C with the ramp rate of the temperature controller programmed at 15 °C/min. After oxidation the rear gold-coated surface was cleaned to remove residual oxide on gold. The samples were then thoroughly degreased and cleaned (using trichloroethylene, acetone, methanol and deionized water) and loaded in the electrochemical cell with platinum counter electrode and Ag/AgCl reference electrode (Fig. 1). The electrical connection of the sample was made on the gold-coated side. The electrochemical etching was carried out in 0.1 M H_2SO_4 medium for 30 min at 10 V potentiostatic bias using a Scanning Potentiostat (PAR Model 362). For photo-electrochemical etching, the oxide surface was illuminated with 400-W UV radiations from a fiber optic wave-guide coupled UV source (Model UV-LQ 400, Dr. Gröbel UV-Elektronik GmbH, Germany). After etching, the samples were washed with deionized water and dried.

The crystallinity of the as-oxidized and electrochemically etched samples was checked by glancing angle X-ray diffraction at different incident angles. The surface morphology of the samples was studied using a scanning electron microscope (Model: JSM 6700F NT) in order to reveal the microstructure of the matrices and the results have been reported [11]. Atomic force microscopy technique was used to determine the surface roughness of the electrochemically etched films using a Digital Nanoscope (Veeco, Multimode SPM).

The semiconducting parameters of the as-oxidized titania films were measured by performing Hall Effect experiments using van der Pauw sample configurations at room temperature with a Lakeshore 7504 Hall measurement setup. Titanium metal was used for the ohmic contacts in this study. Similar experiments were performed with the porous titania samples.

The porous templates obtained after electrochemical etching were then contacted with 3 mm diameter palladium dots to fabricate Pd/ TiO_2 /Ti–Au vertical sensor configurations. The detailed sensor study with this structure in 500 and 1000 ppm hydrogen and at different temperatures (200–400 °C) has been reported [11] by us.

3. Results and discussions

3.1. Glancing angle X-ray diffraction study

The crystallinity of the as-oxidized titania surface was studied using glancing angle X-ray diffraction technique at different incident angles (0.2° , 0.5° , 1° and 10°). The GAXRD patterns are shown in Fig. 2(a). The incident angle was varied from grazing incidence (0.2°) to a high value (10°) in order to get an idea of the variation in stoichiometry of the oxide matrix along the depth of the films. The incident angle variation changes the penetration depth of X-rays which increases with the increase in the value of the incident angle. The XRD patterns shown in Fig. 2(a) indicate that for low incident angles, the intensity of the surface rutile TiO_2 peaks is higher relative to the Ti_xO phases ($\text{Ti}_x\text{O} \equiv \text{Ti}_3\text{O}$ and Ti_6O). Basically Ti_3O and Ti_6O are titanium rich non-stoichiometric oxide phases and are isostructural to titanium. The isostructural property of these oxide phases is inferred from the 2θ positions of their reflections in the XRD patterns and that of Ti, when compared with the standard JCPDS files. The probable reason for the surface of the samples to be rich in TiO_2 and the bulk with Ti_xO is that the surface was exposed to higher partial pressure of oxygen during oxidation and the oxidation of the bulk depends primarily on the extent of diffused oxygen. The diffusion of oxygen in the bulk is expected to be less and hence the underlying titanium layers are partially oxidized. Also there

was no indication of aluminium oxide in the GAXRD patterns implying low (doping) concentration of aluminium, distributed in the TiO_2 matrix. This can be explained from the procedure followed during oxidation. The oxidation process was initiated at 800°C by introducing oxygen into the furnace and an inert atmosphere was maintained using high purity argon until the temperature reached 800°C . This prevented the initial oxidation of aluminium to aluminium oxide, expected due to its strong oxygen-affinity. However, there might be some partial diffusion of aluminium into the titanium substrates under this temperature condition. As a result the quantity of aluminium is reduced on the surface of the substrates to some extent. During oxidation of the titanium substrates at 800°C , aluminium enters substitutionally into the titanium dioxide lattice and Al^{3+} ions replace Ti^{4+} due to smaller ionic radius of aluminium [12]. Since aluminium is distributed in the titanium substrates the clustering of excess unreacted aluminium oxide along the grain boundaries of titanium dioxide on the surface is prevented. This is also evident from the oxide diffraction patterns (Fig. 2(a)) as there is no aluminium oxide peak for all four incident angles. This result apparently implies that aluminium is present in very low concentration but the uniformity of the aluminium distribution along the depth in the TiO_2 matrix cannot be ensured. Nevertheless, the GAXRD results indicate that the matrix is non-stoichiometric although there is difference in stoichiometry between the surface and the bulk. Since non-stoichiometry is the sole cause of

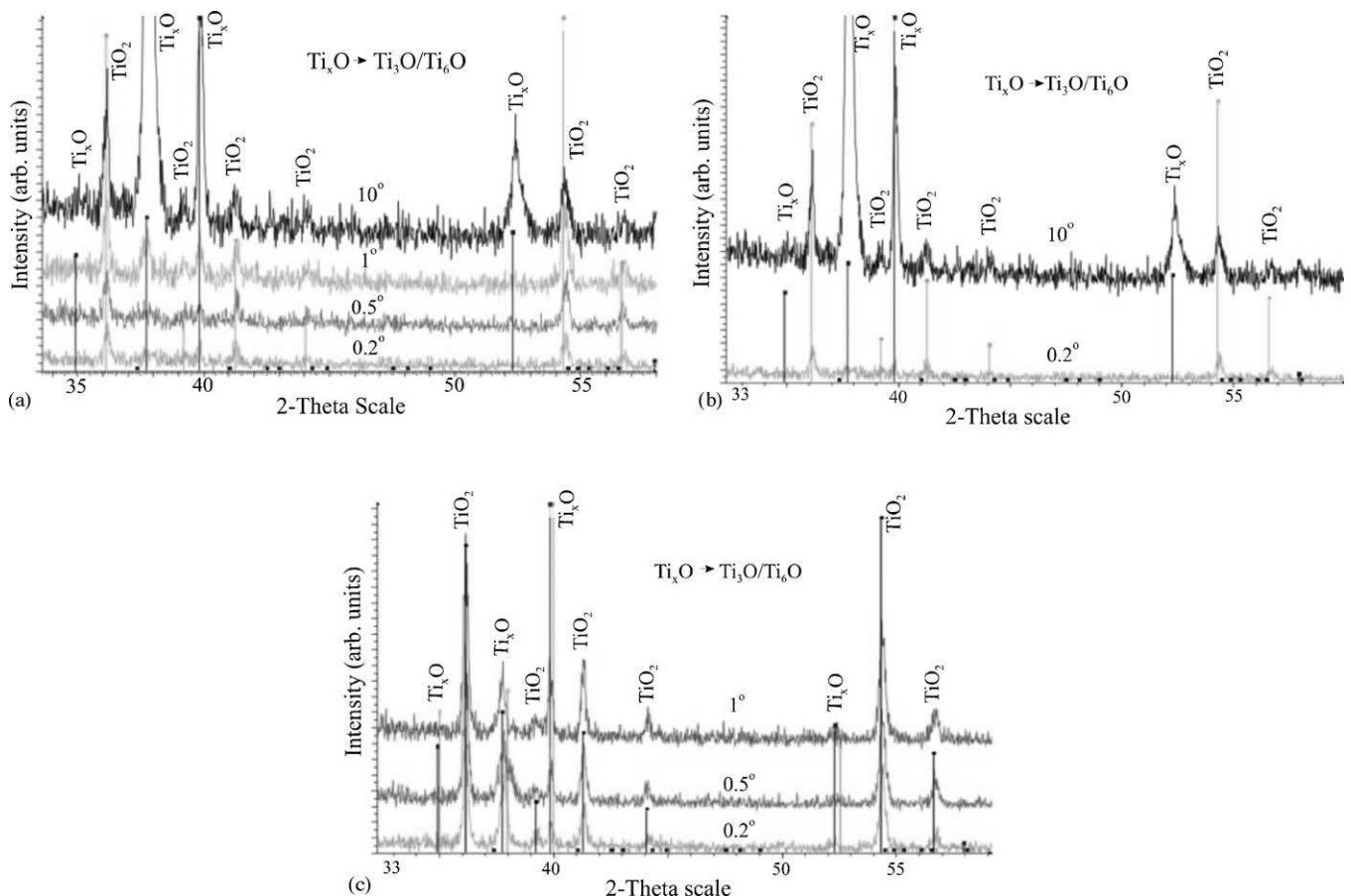
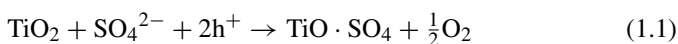


Fig. 2. GAXRD patterns of: (a) the as-oxidized surface; (b) the dark etched surface; (c) UV light etched surface.

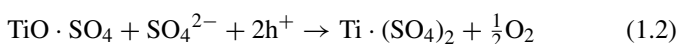
conductivity in titanium dioxide this may also lead to the variation in the conductivity between the surface and the bulk.

The glancing angle X-ray diffraction patterns of the electrochemically etched titania films in absence of UV light are shown in Fig. 2(b). The diffraction patterns were recorded at two different incidence angles (0.2° and 10°) for a comparative analysis of the surface and bulk compositions, respectively. The XRD patterns shown in Fig. 2(b) reveal that the intensity of the surface rutile TiO_2 peaks is higher relative to the Ti_xO phases ($\text{Ti}_x\text{O} \equiv \text{Ti}_3\text{O}$ and Ti_6O) for grazing incidence (0.2°), like that of the as-oxidized surface. In fact, the intensity of the Ti_xO phases is almost negligible for 0.2° glancing incidence. This implies that the surface and bulk compositions of the grains remain almost the same as that of the as-oxidized matrix. Probably in this case the polycrystalline surface has been selectively etched along the grain boundaries without any compositional change, which needs further confirmation by other studies.

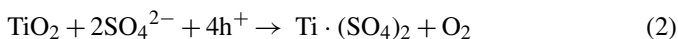
GAXRD studies were also initiated with the samples etched in presence of UV light. For these samples the nature and composition of the surface was studied, in order to get an idea of the etching rate. Hence, the GAXRD studies were performed only at low incident angles (0.2° , 0.5° and 1°) (Fig. 2(c)). From Fig. 2(c) it is evident that for grazing incidence (0.2°) the intensity of the Ti_xO phases has increased to a great extent, contrary to the earlier cases. This probably implies that the bulk layers have been exposed as a result of photo-electrochemical etching. Basically the electrochemical etching is a hole governed process in which the grain boundaries or the bulk grains are selectively dissolved and a typical etching pattern appears on the oxide surface [9]. UV exposure during etching enhances the etching rate by generating excess holes in the titania energy band. The potentiostatic etching reactions proceed as follows:



where ' 2h^+ ' are positively charged holes.



Adding Eqs. (1.1) and (1.2),



As the etching progresses the oxide is lost from the surface and a porous morphology is developed. The band gap of titania is ~ 3.2 eV and the peak wavelength of the UV radiations used is ~ 350 nm. Hence, UV photo irradiation of the oxide surface can generate free charge carriers (holes in the valence band and electrons in the conduction band) in the oxide matrix. This facilitates the etching process by enhancing the etching rate using the excess holes generated in titania band with UV exposure (Eq. (2)). Hence, etching in presence of UV light is more vigorous and can affect the surface of the grains along with the selective dissolution of the grain boundaries. In fact, the direction of electrochemical etching is difficult to predict for polycrystalline surfaces. The basic criterion for good directional potentiostatic etching in acid medium is high crystallinity of the starting material. So the bulk layers are now exposed to the glancing incidence X-rays as a result of photo-electrochemical etching leading to

very high intensity Ti_xO phases in the diffraction pattern at 0.2° incidence. However, due to the enhancement in the rate of electrochemical etching in presence of UV light it is expected that the surface porosity of the samples will be higher relative to the dark etched samples. The other two patterns at 0.5° and 1° incident angles in Fig. 2(c) reveal the stoichiometric information about the sub-surface layers and it is seen that the intensity of the Ti_xO phase is also quite significant in the patterns.

3.2. Morphological studies: SEM and AFM

The scanning electron microscopic study of as-grown oxide surfaces and electrochemically etched surfaces in absence and in presence of UV light was performed to get an idea of the variation in surface porosity due to etching. The detailed SEM study has been reported elsewhere [11]. The scanning electron micrographs revealed the polycrystalline nature of the oxide surfaces and the porous morphology developed after electrochemical etching. The variation in grain size between the as-oxidized surface and the electrochemically etched surfaces was also evident from this study. The grains were tetragonal in shape and the average grain size of the distinctly separated grains on the as-oxidized surface was ~ 300 – 330 nm. The size of the tetragonal rutile grains was reduced upon etching in acid medium under potentiostatic bias. The grain size on the dark etched oxide surface was in the range ~ 115 – 140 nm. For the UV light etched surface the grain size was widely varying in the range ~ 100 – 250 nm. The relative increase in the grain size implies a possibility of grain growth during etching in presence of UV light. This is attributed to the vigorous etching rate attained upon UV exposure. As mentioned earlier, in presence of UV light etching rate is relatively higher due to the supply of excess holes. Hence, it is quite likely that after a certain time the underlying titanium layers of the substrate may be exposed to the etching solution under potentiostatic bias. In this situation the reverse process occurs and titanium metal is anodically oxidized to titanium dioxide in 0.1 M sulphuric acid medium. The oxide newly formed will adhere to the skeleton porous structure by getting deposited along the grain boundaries immediately after its formation. This may lead to non-uniform increase in the size of the grains.

From the SEM study it was evident that the relative porosity (and hence the exposed surface area) in the oxide matrix after etching in UV light was more, which makes it a more suitable substrate for the fabrication of hydrogen sensitive structures. This was further verified by calculating the surface roughness values for the dark etched and UV light etched surfaces from atomic force microscopy studies. Figs. 3 and 4 represent the AFM pictures of the electrochemically etched surfaces in absence and in presence of UV light, respectively. The rms roughness of the samples etched in absence of UV light is 36.309 nm and is increased to a value 123.04 nm when the samples are etched in presence of UV light. This apparently implies that the etch pits are deeper and are frequently repeated on the surface. Basically surface roughness is defined as the change in the profile of the surface in which the height and the depth of ridges and valleys vary in the nanometer order. From the

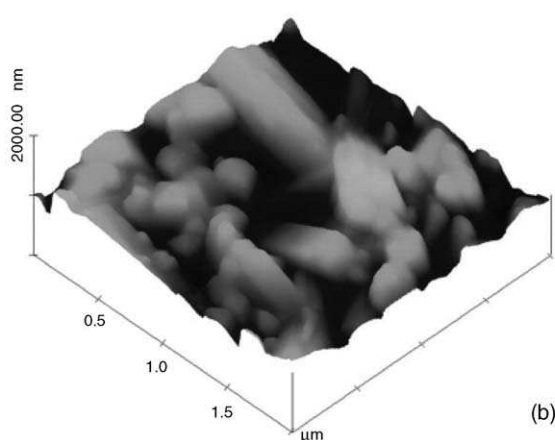
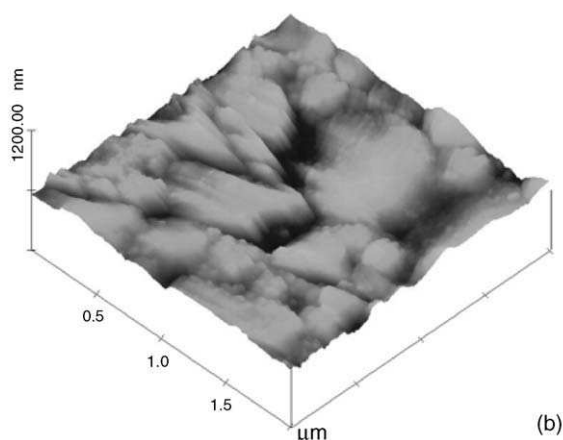
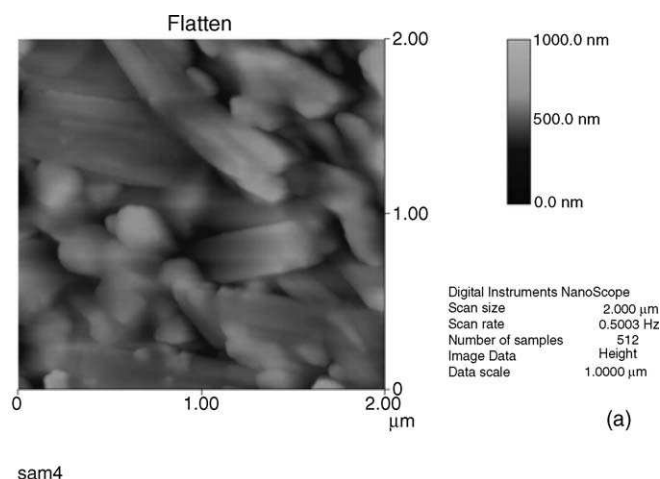
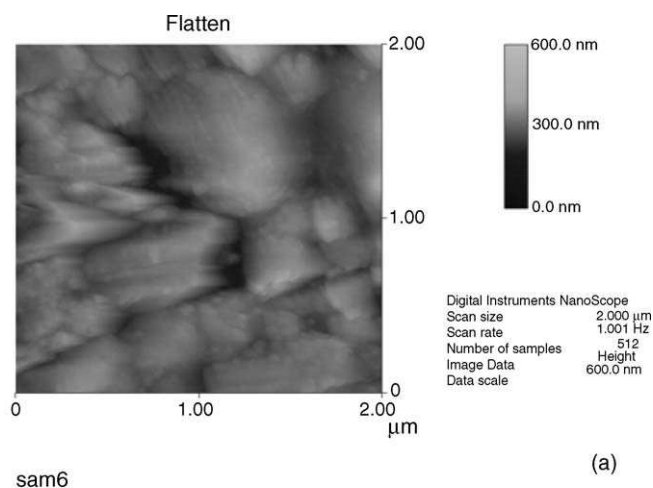


Fig. 3. AFM: (a) topography and (b) surface image of the etched titania surface (without UV light).

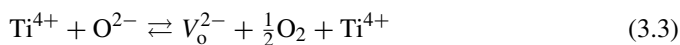
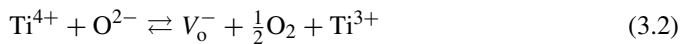
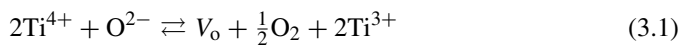
Fig. 4. AFM: (a) topography and (b) surface image of the etched titania surface (with UV light).

AFM topography shown in Fig. 3(a) the maximum height of a ridge/hill is 600 nm. This implies the minimum depth of the valley/pit is also 600 nm by considering the surface comprising of the top of the ridges/hills. For the samples etched in presence of UV light the minimum depth as seen from Fig. 4(a) is 1000 nm based on the same argument. Hence, the porous channels are deeper in case of the UV light etched surfaces. Considering the width of the ridges/hills in Figs. 3(b) and 4(b) for both categories of samples, it is seen that the average width for the UV light etched surface (~ 522 nm) is relatively less than the dark etched surface (~ 590 nm). However, from the figures it is also evident that there is variation in the width of the ridges/hills due to non-uniform etching. So the average ratio h/w (height/width) of a ridge/hill is more for the samples etched in presence of UV light. Mathematically the ratio h/w can increase either with the increase in height or decrease in width of the ridges and in this case 'h' increases and 'w' decreases, for the samples etched in presence of UV light. Since the increase in 'h' is relatively more than the change in 'w', it is apparent that the etching direction is perpendicular to the surface, i.e. biased along the depth of the oxide films. Nevertheless, it is a cursory statement regarding the etching direction based on the randomly oriented grains in the starting oxide matrix. Further studies are required to specify the etching direction.

3.3. Electrical studies: resistivity and Hall Effect

Titanium ohmic contacts were deposited on the as-oxidized titanium dioxide surface for the resistivity and Hall Effect studies. Although the intercontact resistance was quite high ($\sim 10^6 \Omega$) linearity was observed in forward and reverse biased I - V characteristics for a pair of titanium contacts, without any pre-annealing treatment. The average value of resistivity measured using van der Pauw technique is $7.88 \Omega \text{ cm}$. The Hall coefficient obtained for a set of five magnetic fields (2–10 kG) was negative, indicating n-type conductivity of the oxide. The average values of carrier concentration and electron mobility as obtained from the Hall Effect measurements are $3.1 \times 10^{15} \text{ cm}^{-3}$ and $227 \text{ cm}^2/\text{V s}$, respectively. The type of conductivity shown by aluminium doped TiO_2 can be analyzed using the ionic model. Pure stoichiometric rutile TiO_2 is an insulator. Extrinsic electronics properties of rutile titanium dioxide depend on lattice defects such as deviations from stoichiometry and foreign ions in the lattice. Non-stoichiometry can be generated either by high temperature hydrogen treatment of the oxide or by the introduction of dopants like aluminium. These non-stoichiometric defects can generate donors or acceptors resulting in n- and p-type conductivity, respectively. Titanium dioxide can be made p-type by intentionally doping the oxide with iron,

aluminium, etc. [13,14]. Nevertheless, pure non-stoichiometric rutile titanium dioxide has extrinsic n-type conductivity due to the defects present in the matrix [14]. The different kinds of defects in non-stoichiometric rutile TiO_2 are: (i) Ti^{3+} at a normal lattice position (electron compensated Ti^{4+} , i.e. an extra electron in the 3d orbital), (ii) oxygen vacancy (V_o), (iii) oxygen vacancy with trapped electron (V_o^-) and (iv) oxygen vacancy with two trapped electrons (V_o^{2-}). These defects are formed during the formation/growth of the oxide. The loss/absence of oxygen from the lattice leading to vacancies/defects can be realized as:

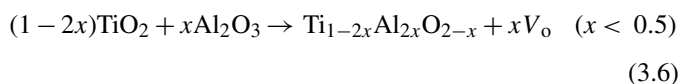


Also the defects can interact with the lattice reversibly in the following manner:

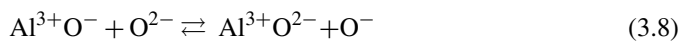
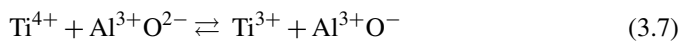


On the application of an electric field the electrons so attached with the vacancies/defects can easily migrate within the matrix thereby leading to extrinsic electronic conductivity. The electron concentration in the oxide matrix is more or less proportional to concentration of such non-stoichiometric defects.

When titanium dioxide is doped with aluminium the oxide becomes non-stoichiometric [12] and the reaction is written as below:



Basically aluminium enters substitutionally into the lattice and Al^{3+} ions replace Ti^{4+} due to smaller ionic radius of aluminium [12]. The following filled/unfilled defect states are expected to be present in the matrix apart from the oxygen vacancies (V_o): (i) O^- in a lattice position (ii) $\text{Al}^{3+}\text{O}^{2-}$ (a filled Al–O level) and (iii) Al^{3+}O^- (an unfilled Al–O level) [14]. The interaction between the lattice and oxygen vacancies as mentioned in Eqs. (3.1)–(3.5) depend on the availability of cationic sites. The other reactions involving aluminium-induced defects are:



The unsaturated O^- in a lattice position is an oxygen ion with a hole in the 2p band. Oxygen has eight electrons in its shells and there are two vacant positions in its outermost 2p orbital. Upon accepting one electron, oxygen becomes O^- with one vacant position in its 2p orbital, which can accept another electron. So O^- can be treated as a hole or an electron acceptor. Hence, aluminium doped rutile titanium dioxide is apparently compensated due to the presence of holes and electrons, later being attached with the vacancies. If aluminium concentration is sufficient the concentration of holes will dominate the electron concentration and the material will be p-type semiconducting under normal

atmospheric pressure (Eqs. (3.7) and (3.8)). It is reported that ~ 0.4 at% Al_2O_3 uniformly dissolves in the rutile matrix [12]. Of course excess aluminium oxide so formed will increase the resistivity and decrease the carrier concentration of the material due to its segregation at the grain boundaries. This was verified by performing experiments with aluminium doped titanium dioxide thin films grown on insulating quartz substrates instead of conducting gold-coated titanium substrates. The oxide thin films were prepared from the Ti–2wt%Al solid solution using the same oxidation technique as outlined in the experimental section. Resistivity and Hall Effects studies were similarly performed with titanium contacts for the films on quartz substrates at room temperature. The measured Hall coefficient for the oxide is positive for a set of five magnetic fields (2–10 kG) indicating p-type conductivity of the matrix. The resistivity, carrier density and mobility values are $1.85 \times 10^3 \Omega \text{ cm}$, $4 \times 10^{12} \text{ cm}^{-3}$ and $424 \text{ cm}^2/\text{V s}$, respectively. The high value of resistivity and low hole concentration is probably due to excess aluminium oxide in the matrix. Since the carrier concentration is low the scattering due to the Coulomb force between the carriers is also low and hence the mobility is quite high. Alternatively it can be reiterated that the presence of large number of aluminium induced defects increases the defect-mobility of this oxide appreciably.

In case the aluminium concentration is less the reactions given by Eqs. (3.1)–(3.5) dominate and the matrix is expected to behave like an n-type semiconductor after some carrier compensation by the minority holes. As discussed in the GAXRD section, the quantity of aluminium present was significantly distributed in the titanium substrates due to the growth conditions. Also the low aluminium concentration was evident from the absence of aluminium oxide peaks in the GAXRD patterns. Hence, in the present study, aluminium doped TiO_2 on titanium substrates will be dominated by non-stoichiometric defects, mainly oxygen vacancies. This attributed n-type conductivity to the grown oxide films. Since the quantity of aluminium is less, the chance of formation of excess unreacted aluminium oxide responsible for higher resistivity is negligible. This argument is substantiated by the low value of resistivity ($7.88 \Omega \text{ cm}$) and relatively high electron concentration ($\sim 10^{15} \text{ cm}^{-3}$) obtained from the measurements.

For the electrochemically etched porous samples (without UV light and with UV light) the Hall measurements at room temperature gave very high electron concentration ($\sim 10^{19}$ and 10^{20} cm^{-3}) and low resistivity ($\sim 10^{-2}$ and $10^{-3} \Omega \text{ cm}$). This apparently indicates near metallic conductivity of the porous samples. Basically the titanium ohmic contacts are expected to propagate deep down the pores (or etched pits) during electron beam metallization and touch the underlying partially oxidized layers. These partially oxidized layers are more conducting than the as-oxidized surface due to their non-stoichiometric composition. Hence, the resistivity and carrier concentration obtained in these cases are that of the bulk conducting layers. The difference in the carrier concentration and resistivity values between dark etched and UV light etched samples is due to high photo-electrochemical etching rate, which exposes deeper metallic (titanium) layers. As a result the ohmic contacts deposited on the surface touch these metallic layers through the pores leading

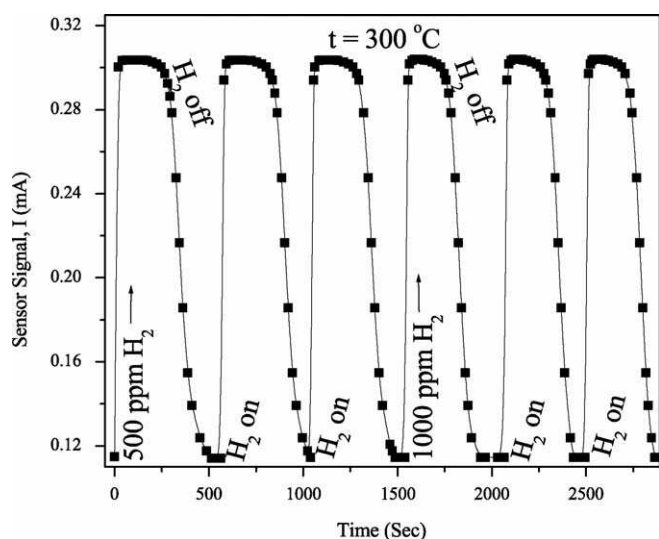


Fig. 5. Transient response pattern of Pd/(porous TiO₂)/Ti–Au sensor structure in hydrogen at 300 °C.

to metallic Hall characteristics. Hence, the electron concentration for the photo-electrochemically etched samples is higher relative to the dark etched samples.

3.4. Hydrogen sensor study

The electrochemically etched samples served as excellent templates for the fabrication of hydrogen sensitive devices with palladium catalytic contact (3 mm diameter and 50 nm thick). The as-prepared templates were insensitive to hydrogen in the temperature range 200–400 °C. The Pd/(porous TiO₂)/Ti–Au vertical sensor configurations (on UV light etched titania surfaces) showed appreciably fast response to 500 and 1000 ppm hydrogen. The best response was obtained at 300 °C for this vertical sensor structure. A typical transient response pattern for the Pd/(porous TiO₂)/Ti–Au sensor structure at 300 °C is shown in Fig. 5. Upon exposure to 500 ppm hydrogen the sensor current increases and then saturates after some time. When the hydrogen pulse is switched off the current decays and gradually saturates near the baseline value. The increase in current upon hydrogen exposure is due to hydrogen adsorption and subsequent release of electrons at the interface by the catalytic palladium layer [15]. The desorption process occurs when the 500 ppm hydrogen pulse is switched off due to reduced partial pressure of hydrogen at the same temperature. The time in which the device current reaches 63% of its saturation value (or the response time) is 5 s at 300 °C in 1000 ppm hydrogen. The detailed sensor study on these porous templates has been reported [11].

4. Conclusion

Porous titanium dioxide films were prepared by thermal oxidation followed by electrochemical etching under potentiostatic

bias at room temperature. The crystalline composition of the grown oxide varies along the depth of the samples, i.e. the deeper layers are more non-stoichiometric relative to the surface. Since non-stoichiometric composition increases the electrical conductivity in oxides the deeper layers are more conducting than the surface. This variation in stoichiometry along the depth is advantageous for the fabrication of vertical electronic devices on titanium dioxide with a low resistive vertical path between two electrical contacts. Also the vertical path resistance between two contacts can be modulated by controlling the etching rate or etching time. The samples etched in presence of UV light shows higher surface roughness relative to dark etched samples which indicates better porous morphology for UV light etched surfaces. The as-grown oxide showed n-type conductivity owing to the dominance of oxygen vacancies over aluminium induced defects. In general n-type conductivity in oxides makes it more favourable for electronic device applications due to low activation energy of the donor states. All these studies reveal that the porous titanium dioxide templates (with increased active surface area) are ideal substrates for gas sensor applications like in electronic nose.

Acknowledgement

S.K. Hazra gratefully acknowledges “Council of Scientific and Industrial Research (CSIR)”, New Delhi, India, for the Senior Research Fellowship.

References

- [1] Yi Hu, H.-L. Tsai, C.-L. Huang, J. Eur. Ceram. Soc. 23 (5) (2003) 691.
- [2] R.D. Shannon, J.A. Pask, J. Am. Ceram. Soc. 48 (1965) 391.
- [3] D. Gong, C.A. Grimes, O.K. Varghese, W. Hu, R.S. Singh, Z. Chen, E.C. Dickey, J. Mater. Res. 16 (2001) 3331.
- [4] O.K. Varghese, D. Gong, M. Paulose, K.G. Ong, C.A. Grimes, Sens. Actuators B 93 (2003) 338.
- [5] O.K. Varghese, G.K. Mor, C.A. Grimes, M. Paulose, N. Mukherjee, J. Nanosci. Nanotechnol. 4 (2004) 733.
- [6] M. Paulose, O.K. Varghese, G.K. Mor, C.A. Grimes, K.G. Ong, Nanotechnology 17 (2006) 398.
- [7] Y. Shimizu, N. Kuwano, T. Hyodo, M. Egashira, Sens. Actuators B 83 (2002) 195.
- [8] T. Iwanaga, T. Hyodo, Y. Shimizu, M. Egashira, Sens. Actuators B 93 (2003) 519.
- [9] T. Sugiura, T. Yoshida, H. Minoura, Electrochem. Solid-State Lett. 1 (1998) 175.
- [10] T. Sugiura, T. Yoshida, H. Minoura, Electrochem. Commun. 67 (1999) 1234.
- [11] S.K. Hazra, S. Basu, Sens. Actuators B 115 (1) (2006) 403.
- [12] K. Hatta, M. Higuchi, J. Takahashi, K. Kodaira, J. Cryst. Growth 163 (1996) 279.
- [13] J. Rudolph, Z. Naturforsch. 14a (1959) 727.
- [14] J. Yahia, Phys. Rev. 130 (1963) 1711.
- [15] D. Briand, H. Wingbrant, H. Sundgren, B. van der Schoot, L.-G. Ekedahl, I. Lundström, N.F. de Rooij, Sens. Actuators B 93 (2003) 276.